European Journal of Wood and Wood Products (2025) 83:133
https://doi.org/10.1007/s00107-025-02281-5

ORIGINAL ARTICLE

Simulation-based assessment of the structural impact response of the Cura Baglama: a drop test approach for wooden stringed musical instruments

H. Kursat Celik[1] · Recep Cinar[2] · Allan E. W. Rennie[3]

Received: 15 March 2025 / Accepted: 30 May 2025
© The Author(s) 2025

Abstract

The Cura Baglama represents the smallest variant within the traditional Turkish baglama family of stringed instruments. Investigating its structural integrity when subjected to sudden impact loading is essential for advancing efforts in standardisation, development, maintenance, repair, and the preservation of its historically significant design characteristics. This study presents a comprehensive analysis of the dynamic structural response of a cura baglama subjected to controlled drop-test scenarios. A reverse engineering methodology, coupled with three-dimensional explicit dynamic analysis, was employed to examine the instrument's behaviour under impact loading. The study evaluated the effects of seven distinct impact positions, simulating a drop from a fixed height of 1000 mm. The simulation results provided critical insights into the instrument's impact response by visualising deformation patterns and equivalent stress distributions across its structure. Regions susceptible to damage were identified by comparing the computed equivalent (von Mises) stress with the material's yield strength, which served as the threshold for irreversible damage. This approach enabled the determination of the critical drop height corresponding to structural failure in each scenario. The findings indicate that, although all scenarios were simulated at a fixed drop height of 1000 mm, Impact Scenario 5 exhibited the lowest calculated threshold for damage initiation, with a critical drop height estimated at 172 mm based on the material yield criterion. These structural impact response analyses offer valuable guidance for instrument designers, facilitating the development of cura baglama models with enhanced strength. While the findings are specific to the analysed instrument model, the methodological approach can be generalised to similar studies. Furthermore, the findings contribute to the broader preservation efforts of these culturally and historically significant musical instruments.

1 Introduction

Music, one of the fundamental aspects shaping human cultural identity, serves as a tangible expression of ancestral tradition, encapsulating the history, beliefs and related values ingrained in societies. The preservation and utilisation of musical instruments play a pivotal role in safeguarding humanity's historical legacy, particularly in live performances (Winternitz 1979). Turkish folk music, deeply rooted in Anatolian culture and the broader Turkic geography, exemplifies the profound connection between music and cultural identity. The baglama, also recognized by its alternate name saz, is deeply rooted in Turkish musical culture, assumes a prominent role in Turkish folk music, symbolising the essence of Turkish culture. The baglama family encompasses diverse stringed instruments in Turkish music, ranging from larger ones like "Meydan Sazı" to smaller members like "Cura" (Yilmaz 2011). Specifically, the Cura Baglama (CB), the smallest member, played by itinerant musicians, holds historical significance in traditional Turkish folk music, offering diverse sounds and playing styles using a plectrum or fingers (Demirbas 2020; Erbil 2021).

✉ H. Kursat Celik
hkcelik@akdeniz.edu.tr

Recep Cinar
recep.cinar@outlook.com

Allan E. W. Rennie
a.rennie@lancaster.ac.uk

[1] Dept. of Agr. Machinery and Technology Engineering, Akdeniz University, 07070 Antalya, Turkey

[2] Elixtek Engineering Software Solutions, Kocaeli, Turkey

[3] School of Engineering, Lancaster University, Lancaster, UK

Published online: 02 July 2025

Skilfully crafted traditional baglamas incorporate various wood types in the construction of their soundboxes, such as mulberry and chestnut, with softwoods like spruce prevailing in the composition of the soundboard. The neck, made from medium-hardwoods like hornbeam or maple, and the bridge exclusively made of maple contribute to the instrument's tone. Nuts and pegs are crafted from hardwoods like ebony or rosewood (Mert 2018). Despite the prevalence of stringed instruments in Turkish music, research on their origin, naming, morphology, development, standardisation, and classification remains limited. Addressing these gaps necessitates analytical research in organology. Detailed studies on the sound formation and structural features of Turkish stringed instruments are notably lacking, leading to a trial-and-error approach in instrument production, revision and/or repair processes without a scientific basis in general (Tetik Isik 2015; Degirmenli 2018).

Stringed musical instruments are delicate and intricate tools susceptible to damage from external forces. Consequently, routine measures should be undertaken to ensure the musical instrument is safeguarded and performs optimally. Musicians and instrument makers must possess a comprehensive understanding of the potential structural vulnerabilities of the instrument, as it may be subjected to various types of damage during its use, transportation, or storage, such as cracks, dents, scratches, or deformation. Possible damages may influence the sound quality, tuning stability, playability, and appearance of the instrument, necessitating costly and time-consuming repairs or replacements. Moreover, certain types of damage may be irreparable.

Mechanical damage in stringed instruments, like the baglama, can occur in various ways, often as a result of physical forces, environmental factors, or mishandling. The headstock, as a structurally vulnerable region, is particularly susceptible to breakage in the event of a fall or exposure to high-magnitude impact loading, which may lead to damage of the sounding components and necessitate repair. Additionally, the joint connecting the neck to the body (soundbox) represents another weak point, and abrupt forces or mishandling can result in fractures or separations, compromising the instrument's structural integrity. Temperature and humidity fluctuations pose further risks. Changes in these environmental factors can cause wood warping, impacting the baglama's shape and playability. Extreme dryness may lead to the wood drying and cracking, while excessive moisture can induce swelling and warping, both jeopardising the instrument's structural integrity. String tension issues, including bridge or nut lifting due to high string tension or inappropriate strings, further influence playability and can lead to additional damage, including string breakage and potential harm to the instrument or adjacent components. Accidental drop cases amplify the risk of damage, potentially causing severe harm to the soundbox, soundboard and neck, resulting in cracks, splits, or complete breakage. Bonds, responsible for the baglama's stability, may also experience breakage, and a hard impact can displace the nut and bridge, affecting playability and intonation. Hence, regular maintenance and careful handling are essential to mitigate these risks and ensure the longevity of the baglama.

Structural deformation analysis of string instruments, particularly under dynamic damage conditions, identifies potential design weaknesses, ensuring strength and sound quality. Techniques like Finite Element Analysis (FEA) are beneficial for such analysis and design optimisation (Carlson 2011). FEA is instrumental in improving the design, construction, and quality of string musical instruments (Celik et al. 2023). It facilitates design optimisation for enhanced sound and strength, ensures quality control for meeting design specifications, enables customisation for individual musicians, and aids in the preservation of historic instruments, thereby enriching the musical experience and preserving cultural heritage (Cook 1995; Kuna 2004; Narasaiah 2008; Kim et al. 2018; Szabó and Babuška 2021; Chakrabarty 2022).

A linear relationship between strain and displacement is assumed, based on a linear elastic analysis with small deformations. However, this presumption remains applicable only within the confines of the small displacement concept. Conversely, when dealing with large displacements, there is a substantial alteration in the initial geometry, necessitating the incorporation of geometric nonlinearity into the solution algorithm (Bhatti 2006). While explicit methods can indeed be applied to linear problems, explicit dynamic analyses are more commonly associated with scenarios involving significant nonlinearities, including large deformations, substantial strains, plastic behaviour, hyperelasticity, and material failure. The explicit dynamics based problem solving approach has proven valuable in addressing scenarios involving sudden impact, such as drop tests (Yan et al. 2010; Wu and Gu 2012; Todorov and Kamberov 2017). This approach is specifically developed and employed for simulating nonlinear structural responses and most especially, in complex engineering problems related to sudden loading, explicit dynamics methods are more suitable, providing an alternative problem-solving procedure (Chang 2007; ANSYS Product Doc. 2023a; Xie et al. 2023). Consequently, it is appropriate to assert that the impact deformation of musical instruments may be considered a nonlinear structural mechanics application covered by the explicit dynamics system.

The literature concerning engineering analysis of string instruments using numerical methods predominantly focuses on modal shape analysis, frequency analysis, and the effect of bridge force (The net mechanical force exerted by the tensioned strings on the instrument's bridge) on the

soundboard component. Specifically, within the realm of plucked or fingered string in bridge for instruments; Quintavalla et al. (2024) examined a Late Baroque Mandolin, providing valuable numerical and visual outputs from FEA. Their work facilitated the identification of mode shapes and the quantification of the effect of structural cracks on the instrument's integrity and acoustics (Quintavalla et al. 2024). Chauhan et al. (2024) analysed the sound radiation patterns of the Sarasvati Veena and the modal behaviour of its top plate. Their findings highlighted the significance of the top plate in influencing the resonator's acoustics over the body of the instrument (Chauhan et al. 2024). Paiva and Dos Santos (2014) conducted modal analysis research on the body of a Brazilian Guitar using engineering simulations and experimental setups. They presented modal shapes of the instrument's body under specified boundary conditions, drawing comparisons between simulation and experimentation (Paiva and Dos Santos 2014). Mansour et al. (2009) investigated a Persian long-necked lute, known as a Setar, by introducing a finite element model. Their study utilised fluid–structure interaction-based simulation results to predict the acoustic effects of modifications to specific parts of the instrument (Mansour et al. 2009). Bielski and Kujawa (2017) explored the non-linear dynamics of guitars through finite element modelling and nonlinear time-domain dynamic (explicit) analyses. Their study aimed to obtain displacement signals and conduct subsequent spectral analyses (Bielski and Kujawa 2017). Stanciu et al. (2020) conducted experimental investigations into the stress and strain states of a guitar's wooden structure resulting from string tension. They underscored the generation of tensile and compression stresses in the guitar body, with higher strain values recorded in the bridge area and at the 8th fret on the guitar neck (Stanciu et al. 2020). Regarding structural analysis, the author's prior publication delved into the deformation behaviour of a Turkish string instrument under various string tensions. This study reported variations in structural stress and deformation maps across the instrument's components due to string tension (Celik et al. 2023).

Despite the prevalence of these issues, there is a lack of comprehensive studies that analyse the effects of accidental drops on the CB. Understanding the potential damage from such incidents can aid in the development of more robust designs and protective measures, contributing to accurate prediction of damage patterns crucial for effective repair and restoration. Especially in the case of drop impact, whether accidental or intentional, it can generate high dynamic loads and large deformations on the instrument, potentially inducing complex failure modes such as permanent local deformation, component fracture, or buckling. Therefore, it is essential to comprehend the dynamic structural response and damage vulnerability of the CB in sudden impact cases (such as drop case) to design effective strategies for its protection and preservation.

As a component of the assessment of structural integrity in a traditional string instrument, this study aims to conduct an impact response assessment of a sample CB against dynamic loading under several drop case scenarios through explicit dynamics FEA. In the study, a reverse engineering approach was employed to create the three-dimensional solid model of the CB, followed by explicit drop test simulations conducted for various impact positions. The study presented visual and numerical outputs obtained from the FEA, encompassing deformation and equivalent stress distributions, impact platform reaction forces as well as internal energy absorption data. The simulation assumes a simplified instrument configuration, wherein strings, frets, and the bridge are excluded to reduce computational complexity. Additionally, due to the absence of well-defined orthotropic failure criteria for the complex wood materials used, all components were modelled using homogeneous linear isotropic properties based on published literature values. The structural outcomes reported herein are specific to the CB model analysed. However, the methodological framework established in this study is generalisable and may serve as a guiding strategy for impact simulation studies in similarly fragile wooden musical instruments.

2 Materials and methods

2.1 Solid modelling procedure

The CB is a musical instrument with structural components crafted from various wood-based materials, such as the soundbox, soundboard, neck, bridge, nut, and pegs, as well as three groups of strings (six cold-drawn steel strings in total, ASTM A228) (Bülbül 2015). The instrument utilised in this study was crafted in 2019 by instrument maker Mr. Dundar Altun in Ankara, Turkey, using handcrafted carving techniques for the soundbox. The key components, such as the soundbox, soundboard, neck and nut were bonded together using hot-melt adhesive, commonly known as bone glue (A traditional adhesive made from animal collagen, prised in instrument making for its strong yet reversible bond and minimal impact on acoustics). Employing a reverse engineering approach and advanced solid modelling techniques, a precise full-scale 3D solid model of the components and instrument assembly was generated. The reverse engineering approach can be handled as a systematic process of analysing a physical object, system, or software to extract design information, functional principles, or construction details—typically when original documentation is unavailable—in order to replicate, modify, or improve the

original. In this process, the physical specimen was subjected to 3D scanning and digitalisation utilising the NextEngine-2020i desktop 3D laser scanner in conjunction with Scan-StudioHD software. Subsequent surface enhancement and supplementary modelling procedures were conducted using SolidWorks 3D parametric solid modelling software. Furthermore, an essential validation criterion for ensuring the accuracy of a 3D model involves comparing the physical mass of the object with the mass of its corresponding 3D digital model. To achieve this, the instrument's mass was measured using a digital scale with a precision of 0.001 g. The determined masses of the physical and digital models were 0.460 kg and 0.465 kg, respectively. These values indicate a high level of success in the 3D solid modelling operation (relative difference: 1%). Figure 1 illustrates the 3D solid modelling procedures, dimensional features, and component details.

2.2 Finite element analysis procedure

2.2.1 Drop test scenarios and boundary conditions

In this study, drop test simulations were conducted assuming seven different impact positions for the instrument. The assumption was made that an individual is carrying the instrument and dropping it onto a relatively rigid platform from a height of 1000 mm while in a static stance. The free fall impact of the instrument was simulated under standard Earth gravity (9.807 m s^{-2}) for the predefined dropping scenarios.

Separately prepared instrument models representing the respective impact positions were generated and subsequently imported into the FEA code for analysis procedures. The original geometric details of each component model imported into the FEA code were preserved. However, strings, frets, and the bridge component were excluded from the simulation, based on the assumption that the strings were not fastened to the instrument during drop scenarios. The explicit dynamics module of the FEA code (ANSYS Workbench), was employed for the drop test simulations.

As shown in Fig. 2, seven drop test scenarios were considered, each representing a distinct orientation of the instrument during free-fall, such as edge-on impact, back impact, and headstock-first impact. The boundary condition was established by taking into account the real-world environment; In real-world use, musicians typically loosen the strings during handling or transport, making the exclusion of string tension in the simulation a valid assumption. Similarly, the frets would have minimal structural impact under dynamic loading conditions described in this study. The bridge, which is not fixed to the soundboard and relies solely on string tension to stay in place, has negligible mass and can be reasonably omitted from the structural analysis without affecting the accuracy of the results. Accordingly, realistic contact conditions were taken into account among the different components. The connections between the components of the instrument were specified as bonded

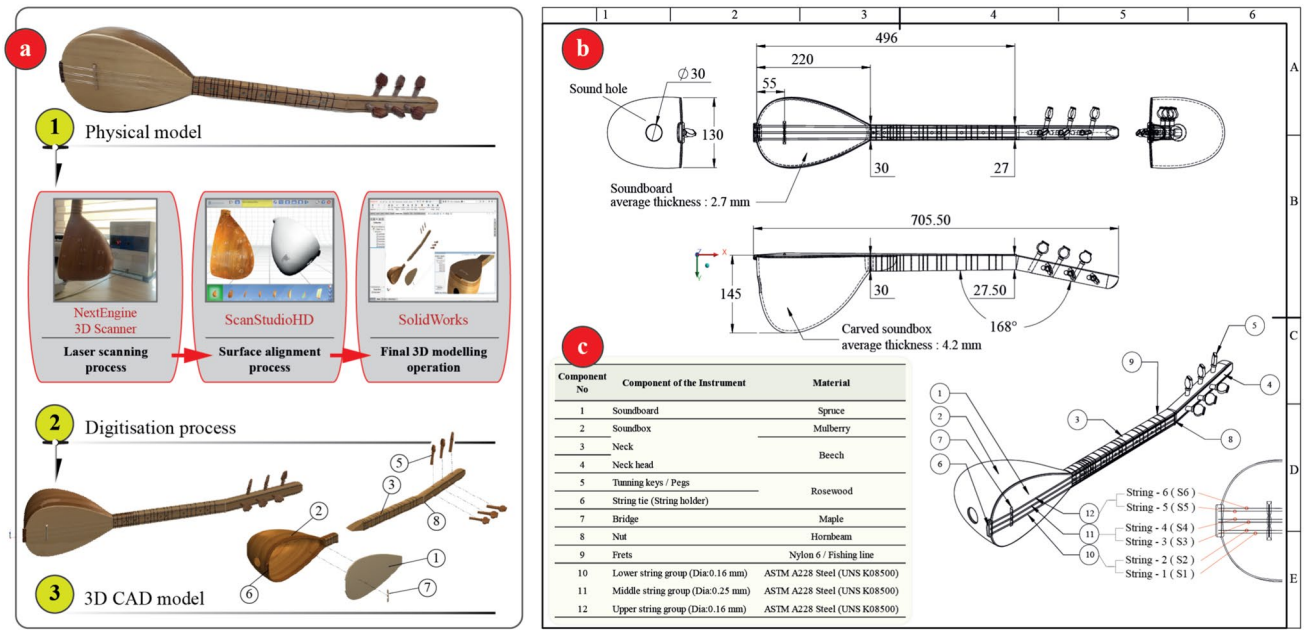

Component No	Component of the Instrument	Material
1	Soundboard	Spruce
2	Soundbox	Mulberry
3	Neck	Beech
4	Neck head	
5	Tunning keys / Pegs	Rosewood
6	String tie (String holder)	
7	Bridge	Maple
8	Nut	Hornbeam
9	Frets	Nylon 6 / Fishing line
10	Lower string group (Dia:0.16 mm)	ASTM A228 Steel (UNS K08500)
11	Middle string group (Dia:0.25 mm)	ASTM A228 Steel (UNS K08500)
12	Upper string group (Dia:0.16 mm)	ASTM A228 Steel (UNS K08500)

1.Soundboard *– The flat top surface that vibrates to produce sound.* ***2.Soundbox*** *– The hollow body that amplifies string vibrations.* ***3.Neck*** *– The long wooden section where the frets and strings are aligned.* ***4.Neck Head*** *– The upper end of the neck that holds the tuning keys.* ***5.Tuning Keys*** *– Pegs used to tighten or loosen strings for tuning.* ***6.String Tie*** *– The point at the bottom where the strings are secured. 7.**Bridge*** *– A small piece on the soundboard that transmits string vibrations.* ***8.Nut*** *– A notched piece at the neck's top that guides the strings.* ***9.Frets*** *– Tied markers on the neck that define musical pitches.* ***10-12.Steel Strings*** *– Metal strings that produce bright, resonant tones.*

Fig. 1 Sample Cura Baglama: 3D solid modelling procedures and the components (**a**), dimensional features (**b**), and component details (**c**)

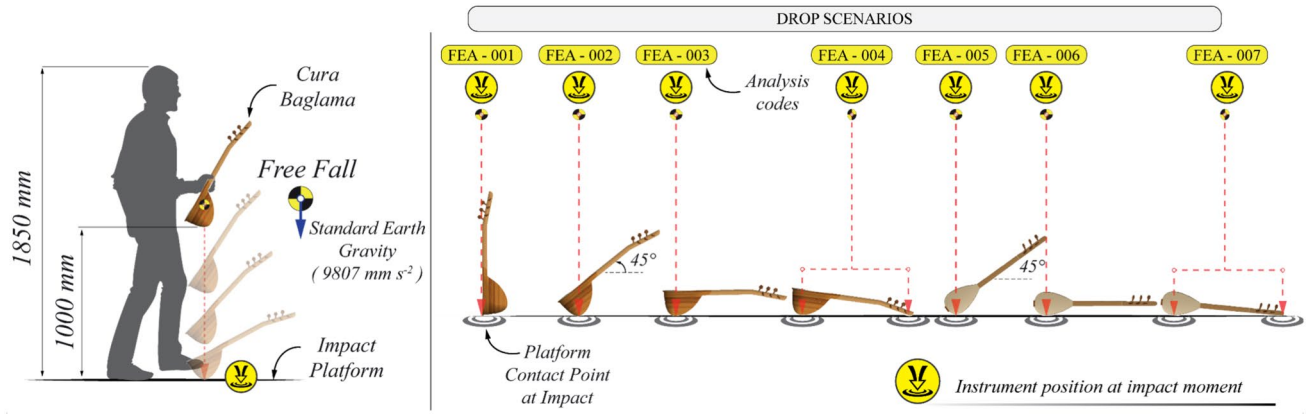

Fig. 2 Schematic depiction of the drop test scenarios

Table 1 Material properties defined in the FEA

Component	Material	Modulus of Elasticity	Poisson's Ratio	Density	Damage Threshold
		(GPa)	(–)	(kg m^{-3})	(MPa)
Soundboard	Spruce (Isotropic)	9.44	0.40	385	31.50
Soundbox	Mulberry (Isotropic)	9.32	0.33	690	48.20
Neck Neck Cover	Beech (Isotropic)	13.90	0.24	710	57.00
Tunning keys / Pegs String tie (String holder)	Rosewood (Isotropic)	13.93	0.37	835	67.20
Nut	Hornbeam (Isotropic)	12.10	0.38	735	50.50
Impact Platform	Structural Steel (Isotropic)	205.0	0.30	7850	250.00

contacts, consistent with the practices in instrument fabrication. Static and dynamic coefficients of friction (0.4 and 0.6, respectively) were assigned to represent the frictional contact conditions between the instrument and the impact platform (McKenzie and Karpovich 1968; Blau 2001; Ross 2010; Mettem 2013). A schematic depiction of the drop test scenarios is presented in Fig. 2.

2.2.2 Material assignment

The individual material properties for each of the assembly components were separately assigned in the FEA. When working with wood, the use of materials exhibiting anisotropic behaviour is often limited by the considerable computational cost and convergence challenges inherent in modelling anisotropic failure, particularly in impact simulations. Consequently, certain assumptions become unavoidable; in this study, a linear isotropic approximation was adopted, in line with previous structural analyses of wood reported in the literature (Mascia and Simoni 2013). The material properties of components were collected from available literature and defined through a homogeneous linear isotropic material model assumption. The material properties were adopted from literature values typically associated with equilibrium moisture contents of 9–12% under room temperature conditions. Moisture effects were not explicitly modelled, which is acknowledged as a limitation. The impact platform was assigned as a steel-based material, a relatively rigid material compared to the instrument's components, in order to clearly observe the impact loading effect caused by free fall reaction forces on the instrument. Table 1 presents the list of the material properties defined in the FEA (Higuchi and Takai 1961; Ross 2010; Meier 2015; Gao et al. 2016; Fu et al. 2017; Obara 2018; Pedrammehr et al. 2018; MatWeb 2023).

2.2.3 Mesh structure details

The mesh structure of the model plays a critical role in determining the simulation results, making it a pivotal step in the pre-processing phase to ensure accuracy. In this regard, curvature-based meshing approaches were implemented using the meshing controls of the FEA module to guarantee precise outcomes (ANSYS Product Doc. 2023b, c). Taking into account the geometry of the components, more precise element sizes were specifically defined for models such as the pegs, nut, and string holder. The optimal element size for the overall mesh structure was determined through preliminary trials. In the study, although a formal mesh convergence plot was not generated, the mesh resolution was selected through iterative pre-processing trials using the curvature-based meshing feature. Skewness analysis was used to assess element quality, and refinements were applied in high-curvature and contact regions. The final mesh yielded an average skewness value, classified as 'excellent',

and maintained acceptable solver times within the limits of the available hardware. The finite element model utilised a combination of automatically selected 4-node tetrahedral (Tet4) and 8-node hexahedral (Hex8) elements, based on geometric region complexity. All elements were first-order and employed full integration, as configured by the ANSYS meshing module for Explicit Dynamics analysis. In the context of an internal verification procedure, a skewness metric was employed to quantify the deviation of elements from equilateral cells. Skewness serves as a practical indicator of element distortion and quality, derived from the Jacobian matrix that governs the mapping between physical and reference domains. A value near zero indicates ideal isoparametric transformation, whereas values approaching one signify severe distortion, i.e. a skewness value of 0 signifies optimal cell quality, whereas a value of 1 indicates fully degenerated cells (0: equilateral; > 0 to 0.25: excellent; 0.25 to 0.50: good; 0.50 to 0.75: fair; 0.75 to 0.9: poor; 0.9 to < 1: bad; 1: degenerate) (Brys et al. 2004; ANSYS Product Doc. 2019). After completing the model processing, the analysis of skewness metrics indicated an average value of 0.249, suggesting that the mesh structure achieved excellent cell quality. Additionally, linear tetrahedral elements with reduced integration were assigned automatically to improve computational efficiency. Hourglass control was automatically applied by the solver. Hourglass energy was monitored and confirmed to remain below 5% of internal energy, indicating that the solution was not adversely affected by hourglass distortions. Detailed information on the generated mesh structure is provided in Fig. 3.

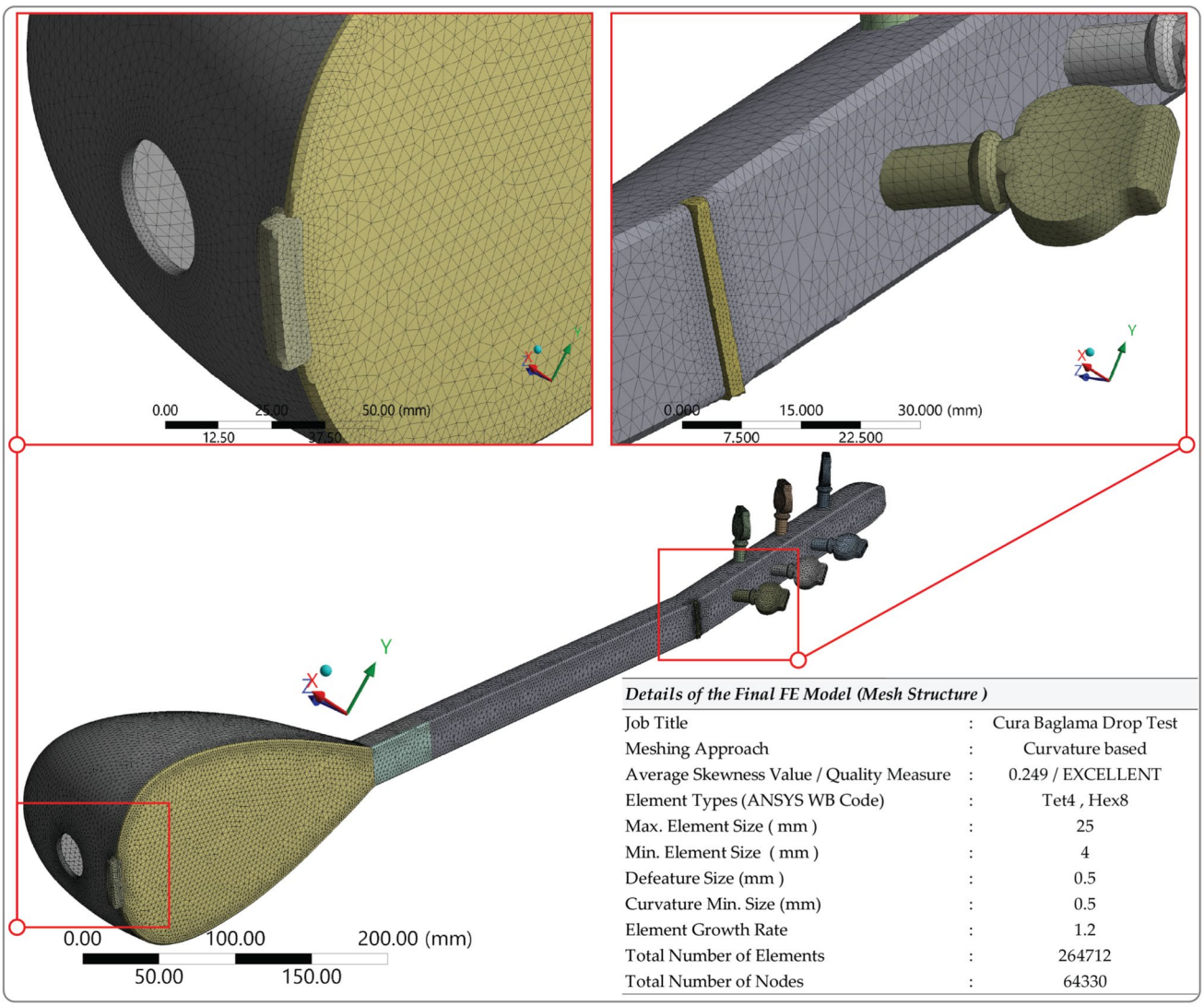

Details of the Final FE Model (Mesh Structure)

Job Title	:	Cura Baglama Drop Test
Meshing Approach	:	Curvature based
Average Skewness Value / Quality Measure	:	0.249 / EXCELLENT
Element Types (ANSYS WB Code)	:	Tet4 , Hex8
Max. Element Size (mm)	:	25
Min. Element Size (mm)	:	4
Defeature Size (mm)	:	0.5
Curvature Min. Size (mm)	:	0.5
Element Growth Rate	:	1.2
Total Number of Elements	:	264712
Total Number of Nodes	:	64330

Fig. 3 Mesh structure details

2.2.4 Solving details

The solving parameters were configured within the explicit dynamics module of the FEA code, incorporating a nonlinear, time-dependent deformation analysis with a small time-step size. The literature on nonlinear FEA studies delves into nonlinearity across three main categories: nonlinearity in boundary conditions (contact), material nonlinearity, and geometry nonlinearity (Wakabayashi et al. 2008; SolidWorks Doc. 2010). This FEA study concentrates on boundary conditions and time dependence in deformation, specifically addressing nonlinearities arising from geometry and contact conditions between the components. The drop test simulation was configured to execute within a time frame of 0.0012 s, carefully considering relevant time intervals associated with impact initiation (full impact-contact cycle), deformation progression (including the peak force), and subsequent rebound (non-contact) phases. This duration enables precise and efficient examination of both system response and energy absorption mechanisms. No additional damping models (e.g., Rayleigh or mass-proportional damping) were introduced. The only energy dissipation mechanisms included were from contact friction and hourglass control. This decision was made to preserve the fidelity of elastic impact modelling and prevent artificial attenuation of the response. The simulation prioritizes investigation into these facets to attain a thorough comprehension of how nonlinear boundary conditions, arising from geometric factors and contact interactions, affect the time-dependent behaviour of the object under analysis. Upon completing the pre-processor steps, the solution processes were executed and documented on a Lenovo ThinkPad P53 series mobile workstation (Intel Core i9-9880H (8C/16 T, 2.3/4.8 GHz, 16 MB), NVIDIA Quadro RTX 4000 8 GB GDDR6, 32 GB DDR4, 2 TB SSD). The simulations were executed using CPU-based parallel processing on a multicore Intel i9 processor. The GPU was not used for solver operations, but assisted in post-processing. ANSYS Explicit Dynamics operates primarily on CPUs, leveraging multithreading for shared-memory parallelism.

3 Results and discussion

3.1 Simulation outputs and interpretation

This study employed a lifelike, precise full-scale 3D model of the CB to conduct drop test simulations. The accuracy of solid modelling, when compared to the physical model, was notably good, revealing a minimal 1% relative variation in mass during the validation of the model. The simulation results effectively illustrated the instrument's deformation behaviour under predetermined drop test scenarios. Furthermore, numerical data on stress and deformation distribution, reaction forces, and energy absorption for related components were successfully extracted.

The failure criterion holds a significant role in strength calculations for designing and analysing musical instruments. This study utilised the Von Mises failure theory, also known as the maximum distortion energy theory (Huda 2022). The damage threshold is identified as the material's yield stress point, marking the limit for irreversible deformation. The Von Mises failure theory, initially formulated for isotropic materials, finds extensive application in engineering scenarios for predicting ductile failure. Its extension to wood, an orthotropic material, offers valuable insights for stress analysis and design considerations. Although widely used in engineering applications, the extension of the von Mises criterion to wood—an orthotropic material—remains a matter of debate, and its applicability continues to be assessed in structural modelling studies (Cabrero et al. 2009).

Simulation results indicate that the highest equivalent stress occurred on the soundboard component in drop test scenario 5, reaching 183 MPa, surpassing the values observed in other scenarios. While the simulation reports peak equivalent stresses as high as 183 MPa in Scenario 5, this value should not be interpreted as a valid post-yield stress but rather as a numerical artefact of exceeding the elastic limit in a linear material model. The yield stress (31.5 MPa) serves as the threshold for irreversible deformation, beyond which the results are no longer physically predictive. In scenario 5, the corresponding reaction force exerted by the impact platform on the instrument was 6252 N, and the internal energy absorbed by the instrument amounted to 2382 mJ. Conversely, the minimum equivalent stress (on the sound box), its corresponding reaction force, and absorbed energy were 65.46 MPa, 4731 N, and 2138 mJ, respectively, in Scenario 3, compared to other scenarios. It is noteworthy that the magnitudes of the reaction forces appear relatively high. This phenomenon can be attributed to the instant dynamic reaction during impact on a point contact case at the impact platform. The simulations were configured with an initial contact condition between the instrument and the impact platform, and a total simulation duration was defined to cover the initial rebound and subsequent non-contact phases. The explicit solver automatically assigned time steps based on the critical stability limit derived from the Courant-Friedrichs-Lewy (CFL) condition. The calculated time increment varied between 2.4×10^{-8} s and 3.1×10^{-8} s, ensuring numerical stability. The total simulation time of 0.0012 s was adequate to fully capture dynamic contact and rebound phases.

It is important to emphasise that the total energy and stress progression align with the reaction force progression during the impact, as illustrated in the corresponding graphs. Empirical calculation of the total energy, based on potential energy considerations (Instrument mass: 0.460 kg, Earth gravity: 9810 mm s^{-2}, Corresponding drop height: 1000 mm), yielded 4513 mJ. In comparison, the simulation output was 4545 mJ, indicating a relative difference of about 0.71%, which serves as a robust validation. To evaluate the accuracy simulation results, a critical aspect involves analysing the energy activity summary as a result of an explicit dynamics simulation study. This summary includes an examination of the energy components, notably internal (absorbed) energy, kinetic energy, contact energy, and hourglass energy activities. The internal energy curve provides insight into energy absorption behaviour, identifying components and drop scenarios that may exceed elastic capacity. The consistency between total input energy and analytically derived potential energy validates the energy fidelity of the simulation. Hourglassing indicates to a form of distortion that does not induce any changes in volume or strain within the corresponding mesh element in a model. Essentially, it signifies an undesirable mode of distortion resulting from the activation of degrees of freedom with zero energy. Consequently, this energy activity is commonly referred to as hourglass energy or zero-mode energy in existing literature (Hallquist 2006; Stewart et al. 2006; Wallmeier et al. 2015). In previous studies, it has been underlined that the hourglass energy should not exceed 5–10% of the internal energy (Björkmon 2010; Dilek and Gedikli 2014; ANSYS Product Doc. 2023a). The energy summaries obtained from the FEA results indicate that the hourglass energy remained below 5–10% of the internal energy values across all simulation scenarios detailed in this study. This suggests that the dimensions of all simulations are adequate, and the mesh structure's precision is deemed satisfactory. Additionally, following peak contact, the simulation transitions into a non-contact (rebound) phase, consistent with elastic impact conditions. This behaviour is characteristic of transient wave propagation in elastic bodies and confirms the occurrence of an imperfect impulse transfer. The presence of this phase provides additional validation for the physical realism of the model.

Figure 4 illustrates the drop test evolution of the simulation results for scenario 1 (FEA-001) in detail. The figure displays the progression of energy conservation, equivalent stress, and reaction force, along with the associated visual stress distribution on the instrument during the impact and rebound phases. Simulation outputs for each drop test scenario are presented in supplementary Figures S1 and, S2, respectively.

The stress magnitudes obtained from the simulations indicated material failure in some of the components, with reference to the material yield stress point. Therefore, a component-based evaluation is crucial for accurately describing the impact effect and damage zones on the instrument. To illustrate this, in addition to visual stress distribution given in related figures, stress and reaction force progression charts for corresponding simulation scenarios have been separately plotted in supplementary Figure S3.

In light of plotted data, another crucial consideration is determining the drop height threshold within the drop test scenarios assumed in this study. Depending on the dropping position, limit (critical) drop heights were calculated by taking into account the yield stress of the materials (Table 2). While all seven scenarios were simulated using a nominal drop height of 1000 mm to evaluate structural response, a subsequent analytical extrapolation was performed to estimate the minimum drop height that would lead to material failure—defined by the material's yield stress. This value, referred to as the 'critical drop height,' was calculated by correlating absorbed energy and stress values with the known yield strength of each component. Among all scenarios, scenario 5 exhibited the lowest critical drop height at 172 mm for the drop position, in conjunction with stress magnitudes of 31.5 MPa, indicating its heightened vulnerability to impact-induced damage. The maximum drop height limit was calculated as 736 mm for scenario 3.

Drop scenarios involving sharp-edge or headstock-first impact orientations resulted in higher stress localisation, underscoring their greater structural vulnerability compared to flat-surface impacts. It can be argued that the descent position significantly influences the occurrence of damage, as a sharp geometric impact is more likely to result in easier damage. The determined limit drop height at the damage threshold, based on the drop position, is presented in Fig. 5.

3.2 Limitations and implications

In string instruments, deformations can substantially influence both the occurrence and quality of sound. Particularly, this research notes that the degree of impairment to specific components of the instrument can have a detrimental influence on sound quality and tuning regulations. This finding was corroborated by the output indicators obtained from simulated damage assessments. Attaining optimal strength and sound quality represents the most challenging aspect of string instrument design. Therefore, conducting a thorough exploration of both the strength and acoustic dimensions of the instruments is imperative to ascertain the optimal parameters for instrument design.

It should be emphasized that this study did not focus on acoustic features but rather on structural integrity in the

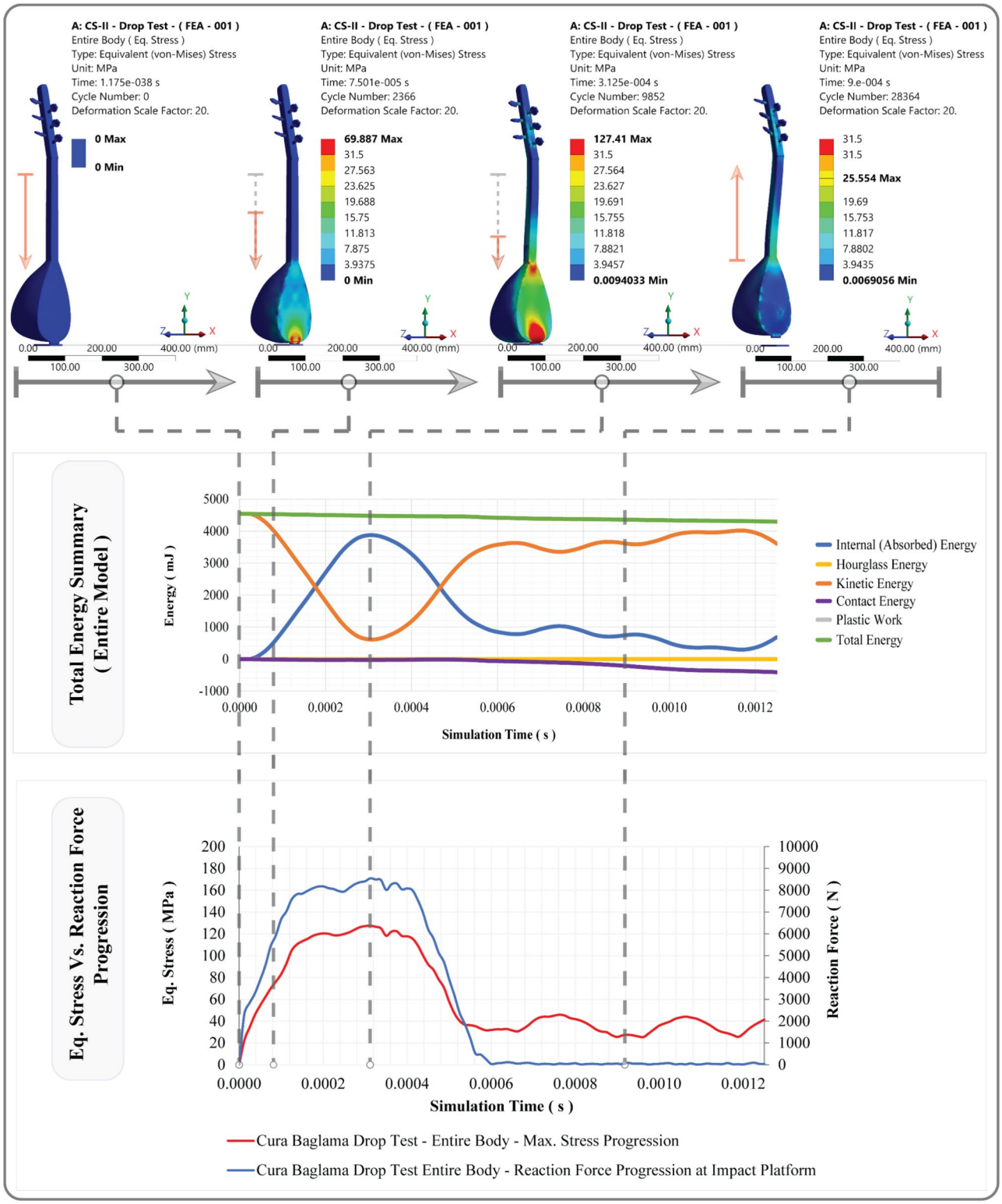

Fig. 4 Simulation results for scenario 1: Energy conservation, equivalent stress and reaction force progressions

Table 2 Calculated limit drop heights at damage threshold (derived from simulation results at 1000 mm nominal drop height)

FEA Code	Component	Drop Height	Corresponding Total (Potential) Energy in the Entire Model	Calculated Max. Eq. Stress / Material Yield Stress by Component	Max. Internal (Absorbed) Energy by Component	Calculated Limit Drop Height at Damage Threshold by Drop Position
		(mm)	(mJ)	(MPa)	(mJ)	(mm)
FEA - 001	Sound Box (Simulation Result)	1000	4545	95.030	871	317
	Damage Threshold (Linearised Result)	507	2305	48.20	442	
	Sound Board (Simulation Result)	1000	4545	99.250	2157	
	Damage Threshold (Linearised Result)	317	1442	31.50	685	
	Neck (Simulation Result)	1000	4545	32.790	535	
	Damage Threshold (Linearised Result)	1738	7901	57.00	929	
FEA - 002	Sound Box (Simulation Result)	1000	4545	109.600	3078	440
	Damage Threshold (Linearised Result)	440	1999	48.20	1354	
	Sound Board (Simulation Result)	1000	4545	34.940	132	
	Damage Threshold (Linearised Result)	902	4098	31.50	119	
	Neck (Simulation Result)	1000	4545	42.670	823	
	Damage Threshold (Linearised Result)	1336	6071	57.00	1099	
FEA - 003	Sound Box (Simulation Result)	1000	4545	65.460	2036	736
	Damage Threshold (Linearised Result)	736	3347	48.20	1499	
	Sound Board (Simulation Result)	1000	4545	12.140	111	
	Damage Threshold (Linearised Result)	2595	11793	31.50	289	
	Neck (Simulation Result)	1000	4545	38.830	354	
	Damage Threshold (Linearised Result)	1468	6672	57.00	520	
FEA - 004	Sound Box (Simulation Result)	1000	4545	94.780	2159	448
	Damage Threshold (Linearised Result)	509	2311	48.20	1098	
	Sound Board (Simulation Result)	1000	4545	28.200	148	
	Damage Threshold (Linearised Result)	1117	5077	31.50	165	
	Neck (Simulation Result)	1000	4545	127.300	1103	
	Damage Threshold (Linearised Result)	448	2035	57.00	494	
FEA - 005	Sound Box (Simulation Result)	1000	4545	71.780	918	172
	Damage Threshold (Linearised Result)	671	3052	48.20	617	
	Sound Board (Simulation Result)	1000	4545	183.000	1298	
	Damage Threshold (Linearised Result)	172	782	31.50	223	
	Neck (Simulation Result)	1000	4545	29.140	467	
	Damage Threshold (Linearised Result)	1956	8890	57.00	913	
FEA - 006	Sound Box (Simulation Result)	1000	4545	57.050	1487	293
	Damage Threshold (Linearised Result)	845	3840	48.20	1256	
	Sound Board (Simulation Result)	1000	4545	107.600	269	
	Damage Threshold (Linearised Result)	293	1331	31.50	79	
	Neck (Simulation Result)	1000	4545	15.280	318	
	Damage Threshold (Linearised Result)	3730	16955	57.00	1185	
FEA - 007	Sound Box (Simulation Result)	1000	4545	48.380	1744	504
	Damage Threshold (Linearised Result)	996	4528	48.20	1738	
	Sound Board (Simulation Result)	1000	4545	57.630	250	
	Damage Threshold (Linearised Result)	547	2484	31.50	137	
	Neck (Simulation Result)	1000	4545	113.100	1239	
	Damage Threshold (Linearised Result)	504	2291	57.00	624	

Red numbers: estimated values; yellow cells: failure-inducing drop height; red cell: overall minimum

context of dynamic impact damage cases. Although acoustic response was not simulated, damage to the soundboard or neck region—especially near the tuning pegs and bridge interface—is known to affect tonal quality and tuning stability in plucked string instruments. In the analysis, the simulation excluded the components of strings, frets, and the bridge, based on the assumption that the strings were not secured to the instrument during drop scenarios. It is important to note that the results might be altered if these components, particularly tensioned strings, were involved.

FEA stands as a valuable tool in understanding material behaviours within structural analyses. However, it is imperative to acknowledge that simulations relying on numerical methods offer only an approximate portrayal of real-world phenomena. Hence, meticulous consideration is warranted to gauge the extent to which simulation outcomes faithfully mirror actual physical circumstances. The most dependable approach for validating simulation results is through their correlation with experimental testing. While experimental validation is not currently available for the Cura Baglama, similar modelling approaches have been adopted in the study of traditional wooden instruments. Future work will incorporate destructive testing and high-speed imaging to support simulation refinement.

In the conclusive assessment of outputs derived from the simulation study, various factors were taken into account.

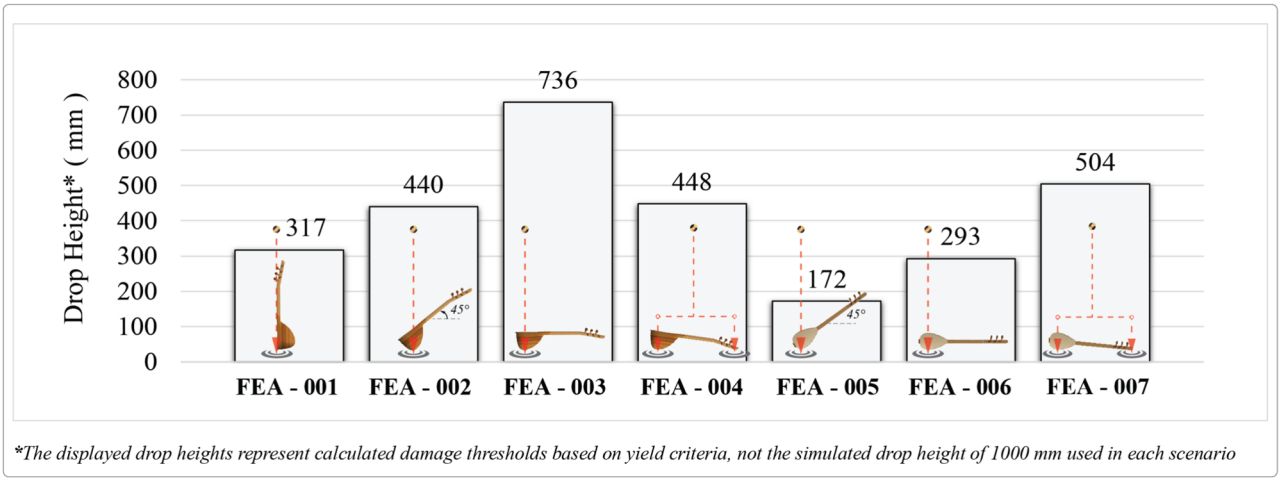

Fig. 5 Determined limit drop height at the damage threshold based on impact position

These factors encompass unforeseen and unpredictable dynamic conditions that might have roles during real operational scenarios, constraints in simulating such conditions, the inherent solution approach specific to numerical methods, requisite assumptions made to tackle these constraints, and an evaluation of the simulation solver platform's capability to rectify any irregularities in the outcomes. Specifically, while the simulation provides insights into the relative severity of drop orientations, its predictive accuracy is constrained by several modelling assumptions. These include the use of linear isotropic materials, the omission of experimental material behaviour and moisture effects, and the absence of model validation via physical drop testing. Therefore, results should be interpreted as indicative rather than definitive.

In spite of the highlighted difficulties, it would be true to say that the analysis showcased a satisfactory portrayal of deformation behaviours under predefined impact positions. The analyses revealed the time-dependent stress distribution patterns and identified high-risk regions based on yield criteria exceedance. While the results align with known structural behaviour in wooden instruments, the accuracy of the damage predictions remains qualitative due to the simplified modelling approach. Despite its simplifying assumptions, the model provides comparative insights into impact response behaviour, including stress localisation patterns and relative energy absorption among components. These insights are valuable for identifying structural vulnerabilities and informing conservative design improvements. Consequently, the simulation results have the potential for valuable applications in the design, production, repair, and standardisation studies of this string instrument.

4 Conclusion

The fabrication and repair of traditional stringed musical instruments necessitate a sophisticated integration of craftsmanship and technical expertise, which should be underpinned by scientific inquiry. In this regard, the present study contributes to the preservation and enhancement of stringed musical instruments, with a particular emphasis on the structural assessment of a specific CB model. By integrating the domains of music, craftsmanship, and engineering, this research advances understanding of how a handcrafted wooden instrument may respond to mechanical impact scenarios—an area of increasing relevance for instrument makers and conservators. Ensuring that such instruments maintain their structural integrity while preserving tonal quality is essential for both their longevity and acoustic performance.

FEA was employed to examine the time-dependent impact response of the analysed CB specimen, focusing on its resistance to mechanical impacts under predefined boundary conditions. The study utilised drop test simulations to investigate impact-induced deformation, yielding findings of potential practical relevance for improving individual instrument design and handling practices. The simulation results identified scenario 5 as the most critical among those assessed, exhibiting the highest equivalent stress values, which corresponded with the greatest reaction force and energy absorption levels. Furthermore, the study estimated a threshold drop height for structural damage initiation in each scenario, with scenario 5 yielding the lowest limit (the critical drop height) at 172 mm. This minimal threshold underscores the susceptibility of the modelled instrument to damage when subjected to impact at specific orientations. Analysis of stress and reaction force progression across different components provided insights into likely material

failure mechanisms and allowed for an estimation of drop height limits that could inform safe handling recommendations. However, given the modelling assumptions—such as the use of linear isotropic material behaviour, the exclusion of string pre-tension, and the idealisation of the impact platform—these thresholds should be interpreted as qualitative indicators rather than definitive design limits. The study also highlights the influence of impact orientation on damage severity, with sharper geometric contact points posing a heightened risk of localised structural compromise. Understanding the response of the studied CB to simulated impact forces contributes to a better-informed design and conservation strategy, albeit within the constraints of the model assumptions. The implications of this research are primarily relevant to stakeholders engaged with instruments of similar scale and construction. Instrument makers may use these findings to explore opportunities for enhancing impact response, potentially through selective reinforcement or improved structural design. Musicians, in turn, may benefit from increased awareness of the instrument's vulnerability to certain types of mechanical stress, informing better handling and transportation practices. Additionally, conservators and caretakers can apply this insight to inform preventive conservation protocols and safe storage guidelines. To extend the model's predictive capability, future studies may: implement orthotropic elasto-plastic material models, use element erosion or progressive failure models, calibrate results using experimental drop test data.

Collectively, the study's findings offer a methodological framework and simulation-based perspective that may inform the preservation of similar traditional musical instruments in fundamental. Nevertheless, further studies—particularly those incorporating experimental validation and advanced material modelling (e.g. orthotropic properties or damage mechanics)—are essential to expand the generalisability of the conclusions and reinforce the structural understanding of historical stringed instruments.

Supplementary Information The online version contains supplementary material available at https://doi.org/10.1007/s00107-025-02281-5.

Acknowledgements This research was partially supported by the Scientific Research Projects Coordination Unit of Akdeniz University (Turkey). The funders had no role in the study's design, data collection, analysis, interpretation, manuscript writing, or the decision to publish. We acknowledge the valuable intellectual contribution of Dr. Sevilay GOK from the Turkish Folk Music Art Branch, Department of Turkish Music, Antalya State Conservatory, Akdeniz University (Antalya, Turkey). The authors declare no conflicts of interest and have no known financial or personal affiliations that could have influenced the reported work

Author contributions H.K.C.: Conceptualisation, Methodology, Resources, Investigation, Visualisation, Formal analysis, Writing original draft R.C.: Software, Data curation, Visualisation A.E.W.R.: Supervision, Project administration, Writing– review and editing.

Funding Open access funding provided by the Scientific and Technological Research Council of Türkiye (TÜBİTAK).

Data availability No datasets were generated or analysed during the current study.

Declarations

Conflict of interest The authors declare no competing interests.

Open Access This article is licensed under a Creative Commons Attribution 4.0 International License, which permits use, sharing, adaptation, distribution and reproduction in any medium or format, as long as you give appropriate credit to the original author(s) and the source, provide a link to the Creative Commons licence, and indicate if changes were made. The images or other third party material in this article are included in the article's Creative Commons licence, unless indicated otherwise in a credit line to the material. If material is not included in the article's Creative Commons licence and your intended use is not permitted by statutory regulation or exceeds the permitted use, you will need to obtain permission directly from the copyright holder. To view a copy of this licence, visit http://creativecommons.org/licenses/by/4.0/.

References

ANSYS Product Doc (2019) ANSYS meshing user's guide: skewness (release 2019 R2). ANSYS Inc., USA

ANSYS Product Doc (2023a) Ansys explicit dynamics analysis guide (release 2023 R2). 280

ANSYS Product Doc (2023b) ANSYS meshing user's guide (release 2023 R1). 556

ANSYS Product Doc (2023c) ANSYS meshing tutorial guide (release 2023 R1). 64

Bhatti MA (2006) Advanced topics in finite element analysis of structures. John Wiley, New York, NY, USA

Bielski P, Kujawa M (2017) Nonlinear modelling in time domain numerical analysis of stringed instrument dynamics. In: AIP conference proceedings. p 020003

Björkmon M (2010) Evaluation of finite element tools for transient structural dynamic simulations of firing systems. Chalmers university of technology

Blau PJ (2001) The significance and use of the friction coefficient. Tribol Int 34:585–591. https://doi.org/10.1016/S0301-679X(01)00050-0

Brys G, Hubert M, Struyf A (2004) A robust measure of skewness. J Comput Graph Stat 13:996–1017. https://doi.org/10.1198/106186004X12632

Bülbül F (2015) Microscopic examination of play-worn steel music strings. Frict Wear Res. 3:1. https://doi.org/10.14355/fwr.2015.03.001

Cabrero JM, Gebremedhin KG, Elorza J (2009) Evaluation of failure criteria in wood members. 2009 Reno, Nevada, June 21 - June 24, 2009. American Society of Agricultural and Biological Engineers, St. Joseph, MI, pp 1274–1280

Carlson M (2011) Application of finite element analysis for an improved musical instrument design. Fender Music Instruments Corp Guitar Prod Res Dev Dep

Celik HK, Gok S, Caglayan N, Rennie AEW (2023) A numerical method-based analysis of the structural deformation behaviour of

a Turkish string instrument (Cura Baglama) under varying string tensions. Appl Sci 13:9682. https://doi.org/10.3390/app13179682
Chakrabarty BK (2022) Integrated CAD by optimization. Springer International Publishing, Cham
Chang S-Y (2007) Improved explicit method for structural dynamics. J Eng Mech 133:748–760. https://doi.org/10.1061/(ASCE)0733-9399(2007)133:7(748)
Chauhan C, Singru P, Vathsan R (2024) Sound radiation patterns of the Sarasvati Veena and their relation with the modal behavior of its top plate. J Meas Eng. https://doi.org/10.21595/jme.2023.23505
Cook RD (1995) Finite element modeling for stress analysis. Wiley
Degirmenli E (2018) An investigation of the sound production in the Turkish musical instrument oud and a proposal for determining the design of stringed instruments from the aspect of their sound characteristics. Gazi University
Demirbas T (2020) Stringed and bowed Turkish folk music instruments in terms of instrumentation. Istanbul Technical University
Dilek D, Gedikli H (2014) Determination of energy absorption characteristics of empty square tailor-welded tubes with finite element method. J Eng Mach 55:56–64
Erbil K (2021) An investigation of the usability of burdur three strings (Üçtelli) Bağlama in Music teaching programs in the line of expert opinions. Necmettin Erbakan University
Fu Y, Fang H, Dai F (2017) Study on the properties of the recombinant bamboo by finite element method. Compos Part B Eng 115:151–159. https://doi.org/10.1016/j.compositesb.2016.10.022
Gao Z, Zhang X, Wang Y et al (2016) Measurement of the poisson's ratio of materials based on the bending mode of the cantilever plate. BioResources 11:5703–5721. https://doi.org/10.15376/biores.11.3.5703-5721
Hallquist JO (2006) LS-DYNA: THEORY MANUAL. 680
Higuchi K, Takai H (1961) Stress-strain diagram, young's modulus and poisson's ratio of textile fibers. J Text Mach Soc Japan 7:4–12. https://doi.org/10.4188/jte1955.7.4
Huda Z (2022) Failures theories and design. 201–213. https://doi.org/10.1007/978-3-030-84927-6_11
Kim N-H, Sankar B V., Kumar A V. (2018) Introduction to finite element analysis and design - 2nd Edition. 552
Kuna M (2004) Finite elements in fracture mechanics. Springer, London
Mansour H, Kasaiezadeh A, Arzanpour S, Behzad M (2009) Finite element modeling of setar, a stringed musical instrument. In: Volume 15: Sound, Vibration and Design. ASMEDC, pp 591–597
Mascia NT, Simoni RA (2013) Analysis of failure criteria applied to wood. Eng Fail Anal 35:703–712. https://doi.org/10.1016/j.engfailanal.2013.07.001
MatWeb (2023) MatWeb: online materials information resource. https://www.matweb.com/
McKenzie WM, Karpovich H (1968) The frictional behaviour of wood. Wood Sci Technol 2:139–152. https://doi.org/10.1007/BF00394962
Meier E (2015) WOOD! Identifying and using hundreds of woods worldwide. The Wood Database
Mert B (2018) "Baglama" with new expression opportunities from the past to the present. Mimar Sinan Fine Arts University
Mettem CJ (2013) Timber bridges. Routledge
Narasaiah GL (2008) Finite element analysis. B.S. Publications
Obara P (2018) Verification of orthotropic model of wood. Arch Civ Eng 64:31–44. https://doi.org/10.2478/ace-2018-0027
Paiva G, M. C. Dos Santos J (2014) Modal analysis of a Brazilian guitar body. ISMA Int Symp Music Acoust Le Mans, Fr 233–239
Pedrammehr S, Aghdam NJ, Pakzad S et al (2018) A study on vibration of setar: Stringed persian musical instrument. J Vibroeng 20:2680–2689. https://doi.org/10.21595/jve.2018.19505
Quintavalla M, Gabrielli F, Canevari C (2024) Acoustical survey and finite element analyses of late baroque mandolin. Int J Wood Cult 3194:1–19. https://doi.org/10.1163/27723194-bja10030
Ross RJ (2010) Wood handbook: wood as an engineering material. U.S. Department of Agriculture, Forest Service, Forest Products Laboratory
SolidWorks Doc. (2010) Solid works simulation premium: nonlinearity training manual document No: 22658021044-ENG0001. USA
Stanciu MD, Bârsănescu P, Goanță V, Savin A (2020) Experimental determination of stress and strain states of the guitar's wood structure. IOP Conf Ser Mater Sci Eng 916:012113. https://doi.org/10.1088/1757-899X/916/1/012113
Stewart JR, Gullerud AS, Heinstein MW (2006) Solution verification for explicit transient dynamics problems in the presence of hourglass and contact forces. Comput Methods Appl Mech Eng 195:1499–1516. https://doi.org/10.1016/j.cma.2005.05.043
Szabó B, Babuška I (2021) Finite element analysis: method, verification and validation, Second Edition
Tetik Isik S (2015) Organology studies in Turkey. Mukaddime 6:197–220. https://doi.org/10.19059/mukaddime.17714
Todorov G, Kamberov K (2017) Virtual prototyping of drop test using explicit analysis. p 020013
Wakabayashi N, Ona M, Suzuki T, Igarashi Y (2008) Nonlinear finite element analyses: advances and challenges in dental applications. J Dent 36:463–471
Wallmeier M, Linvill E, Hauptmann M et al (2015) Explicit FEM analysis of the deep drawing of paperboard. Mech Mater 89:202–215. https://doi.org/10.1016/j.mechmat.2015.06.014
Winternitz E (1979) Musical instruments and their symbolism in western art, 2nd edn. Yale University Press, Connecticut (USA)
Wu SR, Gu L (2012) Introduction to the Explicit finite element method for nonlinear transient dynamics. John Wiley and Sons
Xie S-C, Kolay C, Feng D-C, Ricles JM (2023) Nonlinear static analysis of extreme structural behavior: overcoming convergence issues via an unconditionally stable explicit dynamic approach. Structures 49:58–69. https://doi.org/10.1016/j.istruc.2023.01.086
Yan YX, Xu WF, Huang XC et al (2010) Numerical simulation on drop test of the conical shell. Appl Mech Mater 44–47:2341–2345. https://doi.org/10.4028/www.scientific.net/AMM.44-47.2341
Yilmaz A (2011) Current changes in professional baglama performance. Halic University

Publisher's Note Springer Nature remains neutral with regard to jurisdictional claims in published maps and institutional affiliations.